Case Studies in Thermal Engineering 27 (2021) 101249

Contents lists available at ScienceDirect

Case Studies in Thermal Engineering

journal homepage: www.elsevier.com/locate/csite

Magneto-free-convection flow of a rate type fluid over an inclined plate with heat and mass flux

Azhar Ali Zafar [a,b], Jan Awrejcewicz [a], Grzegorz Kudra [a], Nehad Ali Shah [c], Se-Jin Yook [d,*]

[a] Department of Automation, Biomechanics and Mechatronics, Lodz University of Technology, 90-924, Lodz, Poland
[b] Department of Mathematics, Government College University, Lahore, 54000, Pakistan
[c] Department of Mathematics, Lahore Leads University, Lahore, Pakistan
[d] School of Mechanical Engineering, Hanyang University, 222 Wangsimni-ro, Seongdong-gu, Seoul, 04763, Republic of Korea

A R T I C L E I N F O

Keywords:
Free convection
Rate type fluid
Magneto-hydrodynamics
Symmetric temperature field
Porous media

A B S T R A C T

On a porous layered inclined plate, magneto-free-convection flow of a rate type fluid is investigated. The problem is modeled as natural convection for oscillating and general movements of an inclined plate moving in a magnetized medium with a slanted external magnetic field that is either stationary or moving in tandem with the plate. The plate is subjected to a symmetric temperature field with double-sided thermal operation. Constant concentration, first order chemical reaction, and thermal conductivity as a general feature of time are used in heat transfer measurement. On the velocity of the fluid, the impact of varying plate angles with the vertical as well as the slanted angle of the magnetic field with the plate are studied. The motion of the plate and temperature distribution in specific situations was discussed. We can retrieve many results by changing the values of the functions and parameters in our general solutions, including the related results for the viscous fluid from the literature as a limiting case. As a result, the matter of identical models is no longer an issue. Furthermore, graphical software is used to do parametric analysis on fluid dynamics.

Where K, mol, m, s, kg, S, W and J stands for Kelvin, mole, metre, seconds, kilogram, siemens, watts and joule, respectively

1. Introduction

Magneto-hydrodynamics (MHD) of electrically conducting fluids have applications in engineering, chemical engineering, and geophysical environments [1,2]. As turbulent stream could be stabilized to the extent that it could be forced to return to a laminar flow using magnetic field and this stabilization could be achieved by coplanar or transverse magnetic fields.

In 1954, Stuart [3] investigated the influence of coplanar and transverse magnetic fields and observed that, if the main fluid's flow direction is parallel to the magnetic lines of force, no interaction takes place unless some deviation or instability arises. In this scenario, a restraining force is induced that is proportional in magnitude but opposite in direction to the velocity component perpendicular to the lines of force. Moreover, it has the tendency to damp out the initial instability. Whereas, when the magnetic field is perpendicular to the flow direction, a change is brought about in the velocity distribution. This may make the fluid flow more stable or unstable to

* Corresponding author.
E-mail addresses: nehadali199@yahoo.com (N.A. Shah), ysjnuri@hanyang.ac.kr (S.-J. Yook).

https://doi.org/10.1016/j.csite.2021.101249
Received 25 May 2021; Received in revised form 30 June 2021; Accepted 13 July 2021
Available online 20 July 2021

Nomenclature

Symbol Units Description
τ [K] Temperature of Fluid
C [mol/m^3] Concentration of Fluid
C_R [s^{-1}] Chemical Reaction Parameter (for first order chemical reaction)
K [m^2] Permeability of porous medium
β_τ [K^{-1}] Thermal Expansion Coefficient
β_C [m^3/mol] Concentration Expansion Coefficient
D_m [m^2/s] Mass Diffusivity
g [m/s^2] Acceleration due to Gravity
ν [m^2/s] Kinematic Viscosity
ρ [kg/m^3] Density of Fluid
λ [s] Relaxation Time
σ [Sm^{-1}] Electrical Conductivity
k [W/m K] Thermal Conductivity
q_r [W/m^2] Heat Flux
c_p [J/kg K] Specific Heat at Constant Pressure
σ [W.m^{-2} K^{-4}] Stefan-Boltzman constant
Pr [dimensionless number] Prandtl-number
R_c [W/m K] Radiation-conduction parameter
Pr$_{eff}$ [dimensionless number] Effective Prandtl number
N [dimensionless number] Buoyancy forces ratio parameter
M [dimensionless number] Magnetic Parameter
Sc d[imensionless number] Schmidt number
q [s^{-1}] Laplace transform parameter
α, β Constants

transition to turbulence so it has a very favorable effect on transition and considerable increase in laminar run could be achieved at the higher values of the magnetic parameter [3–5].

A self-sustained flow driven by the presence of a temperature gradient is known as natural or free convection flow and it is one of the important modes of mass and heat transfer in many technological and geophysical phenomena. A comprehension of the laminar-turbulent transition in such flows will help to control and forecast the heat transfer rate [6].

At present, several researchers have focused their attention on the application of magnetic fields in the dynamical systems. Moreover, free convection flow models under the influence of magnetic field have been in high demand in energy generators specifically in MHD generators, polymer fabrication, power elevators, aerodynamic heating, purification of mineral oil and metallurgical processing [7,8]. For notable citations regarding the heat and mass exchange with MHD flows we refer to Refs. [9–15].

In most of the investigations regarding MHD natural convection flows, it is important to note that the external magnetic field is fixed to the fluid. But Narahari and Debnath [16] investigated MHD-free convection flow considering two cases:

i. The magnetic field is stagnant relative to the fluid (MFSRF),
ii. The magnetic field is stagnant relative to the plate (MFSRP).

Later on, Shah et al. [17,18] extended the results for the case of varying wall temperature and a chemical reaction on the plate along with the cases MFSRF and MFSRP.

Transition to turbulence and instability of natural convection on inclined plates are important as they are associated with thermal stratifications in heat exchangers and cryogenic tanks etc. Among many investigations regarding natural convection flows on inclined plates, Sparrow and Husar [19] reported the generation of longitudinal vortices in the natural convection flow of water on an inclined plate. For more related works for the case of natural convection on inclined plates for viscous fluid see Refs. [20–23].

Due to many practical applications of porous medium, for instance: its use in solar water desalination systems to boost water condensation or evaporation, its use as an insulator (for all temperature ranges) and as a heat transfer promoter motivated the engineers and hydrologists to examine the fluid flows in porous materials ranging from sand packs to fused Pyrex glass in order to calibrate their reactions in several types of reservoirs [24].

The requirements of modern technology have motivated the interest of researchers in fluid flow studies, to investigate the interaction of several phenomena. One of these phenomena is certainly flow of electrically conducting fluid through porous medium in the present of magnetic field.

Darcy [25] seems to be among the pioneers who initiated the mathematical theory of the flow of fluid through a porous medium. For the case of steady flows, he made the assumption that the viscous forces are in equilibrium with external forces due to pressure difference and body forces. The free as well as forced convection flows through permeable medium and channels are much significant in scientific and engineering domains that encompasses earth science [26], nuclear engineering [27] and metallurgy [28,29].

Cunningham and Williams [30] pointed out many geophysical applications of dynamics of fluids in porous media. McWhirter et al. [27] presented the experimental results of the MHD flow in a porous medium necessary for designing a blanket of liquid metal around a thermonuclear fusion-fission hybrid reactor. Moreover, results presented by Prescott and Incropera [28] and Lehmann et al. [29] show that during the solidification process of the metallic liquid, the intensity of the interdimeric flow in the porous medium is influenced by the applied permanent magnetic field.

Some notable studies of MHD heat mass transfer with porous medium can be found in the references [31–39].

The research outcomes of the fluid models with multiple applications cannot be achieved by considering just viscous fluids, so fluids with additional properties need to be investigated and, in this regard, non-Newtonian fluids are proven to be more appropriate in emerging and modern technologies. Among different classes of non-Newtonian fluids, rate type fluid models in general and Maxwell fluids in particular are more practical as they consider both memory and elastic effects. This model was first introduced by Maxwell to predict the viscos-elastic characteristics of air [40]. Despite the usefulness of non-Newtonian fluids, the nonlinear relation between shear rate and shear stress makes the flow equations more complex and to handle such flow equations is not trivial. Therefore, a very few efforts have been made for the research related to the MHD-free-convection considering the rate type fluids, see for example [41–43] but it is important to mention that they only correspond to the case when magnetic field is stagnated with respect to the fluid.

Maxwell fluids are one of the important classes of rate type fluids. In fact, Maxwell fluid is a viscoelastic fluid having the properties both of elasticity and viscosity. This class of fluids is named for James Clerk Maxwell who proposed the model in 1867. The Maxwell fluid model was originally developed with an aim to describe the elastic and viscous response of air [40]. Nowadays, it is; however, frequently used to model the response of various viscoelastic fluids ranging from polymers to the Earth's mantle.

Motivated with these above-mentioned investigations, the aim of this manuscript is to investigate the MHD free convection flow of Maxwell fluid on a porous layered inclined plate. Further, the plate is exposed to double-sided heat action of surrounding environment temperature and a slanted magnetic field that is held stagnated either with respect to the fluid or to the plate. More exactly, our interest is to bring to light the influence of the inclination of the plate and the slanted angle of the magnetic field on the dynamics of the fluid. Moreover, by customizing the values of inclination of the plate and slanted angle of the plate we can discuss the cases for horizontal/vertical plate and coplanar and transverse magnetic field influences, respectively. In our model, we are considering the general motions of the plate and temperature distribution of the plate governed by general function of time. Selecting different values of the functions and parameters in our general solutions, we can recover several results including the corresponding results for the viscous fluid from the literature as limiting case. Consequently, the problem related to similar models is completely solved. Finally, the effects of the parameters on the velocity of the fluid over moving plate and temperature distribution are also investigated and useful conclusions are reported.

2. Problem statement

Consider the unsteady free convection flow of an electrically conducting incompressible Maxwell fluid over an inclined porous plate. The x-axis is taken as vertical, and plate is making an angle γ with it and $0 \leq \gamma \leq \frac{\pi}{2}$. Moreover, the plate is non-conducting and having infinite length. A uniform magnetic field of strength $\overrightarrow{B} = (B\cos\vartheta, B\sin\vartheta)$ is applied slanted to the plate with slant angle ϑ, further with the provision that other held magnetic field is fixed to the fluid or to the plate. At the beginning, fluid and plate are stationary having constant temperature τ_∞ and species concentration C_∞.

After the time $t = 0^+$, temperature varies according to the relation $\tau_\infty + \tau_w f(t)$ and concentration is maintained at the constant value C_w. Moreover, the plate starts to excel with certain velocity $F_o g(t)$. Here, F_o is a constant having dimension of velocity and $f(\cdot)$, $g(\cdot)$ are piecewise continuous functions that diminish at $t = 0$.

2.1. Geometry of the problem

Adopting the usual Boussinesq's approximation, neglecting the viscous dissipation and Joule heating effects, assuming the induced magnetic field is imperceptible in contrast to the applied magnetic field and following [41,42] the governing equations for Maxwell fluid flow model related to shear stress and magneto-free convection and thermal radiations are given by the following system of partial differential equations (PDEs)

$$\frac{\partial F(y,t)}{\partial t} = \frac{1}{\rho}\frac{\partial S(y,t)}{\partial y} + g\beta_\tau(\tau-\tau_\infty)\cos(\gamma) + g\beta_C(C-C_\infty)\cos(\gamma) - \frac{\nu}{K}F(y,t) - \frac{\sigma B^2 \sin^2\vartheta}{\rho}F(y,t), \tag{1}$$

$$\left(1+\lambda\frac{\partial}{\partial t}\right)S(y,t) = \mu\frac{\partial F(y,t)}{\partial y};\ y,\ t > 0, \tag{2}$$

where $F(y,t)$denotes the velocity of the fluid and $S(y,t)$ is the shear stress.

Eq. (1) is valid if the magnetic lines of forces are stagnated relative to the fluid, if the magnetic lines of forces are stagnated relative to the plate, then Eq. (1) is replaced by [16,17,47].

$$\frac{\partial F(y,t)}{\partial t}=\frac{1}{\rho}\frac{\partial S(y,t)}{\partial y}+g\beta_\tau(\tau-\tau_\infty)\cos(\gamma)+g\beta_C(C-C_\infty)\cos(\gamma)-\frac{v}{K}F(y,t)- \\ -\frac{\sigma B^2\sin^2\vartheta}{\rho}(F(y,t)-\varepsilon F_o g(t));\ y,\ t\ >0. \tag{3}$$

In the above expression, the parameterε is 0 and 1 for MFSRF and MFSRP, respectively.
Eliminating $S(y,t)$ from (3) by using (2), we get

$$\left(1+\lambda\frac{\partial}{\partial t}\right)\frac{\partial F(y,t)}{\partial t}=v\frac{\partial^2 F(y,t)}{\partial y^2}+\left(1+\lambda\frac{\partial}{\partial t}\right)(g(\beta_\tau(\tau-\tau_\infty)\cos(\gamma)+\beta_C(C-C_\infty)\cos(\gamma))- \\ -\frac{v}{K}F(y,t)-\frac{\sigma B^2\sin^2\vartheta}{\rho}(F-\varepsilon F_o g(t))\bigg). \tag{4}$$

Further, heat and concentration equations are

$$\rho c_p\frac{\partial\tau(y,t)}{\partial t}=k\frac{\partial^2\tau(y,t)}{\partial y^2}-\frac{\partial q_r}{\partial y}, \tag{5}$$

$$\frac{\partial C(y,t)}{\partial t}=D_m\frac{\partial^2 C(y,t)}{\partial y^2}-C_R(C-C_\infty), \tag{6}$$

With the boundary and initial conditions

$$F(0,t)=F_o g(t),\tau(0,t)=\tau_\infty+\tau_w f(t),C(0,t)=C_w;\ t\geq 0, \tag{7}$$

$$F(y,t)<\infty,\tau(y,t)\to\tau_\infty,C(y,t)\to C_\infty \text{ as } y\to\infty. \tag{8}$$

$$F(y,0)=0,S(y,0)=0,\tau(y,0)=\tau_\infty,C(y,0)=C_\infty;\ y\geq 0, \tag{9}$$

By adapting (for an optically thick fluid) the Rosseland diffusion approximation [44,45].

$$q_r=-\frac{4}{3}\frac{\sigma}{R_k}\frac{\partial\tau^4}{\partial y}, \tag{10}$$

And for the case $|\tau-\tau_\infty|<<0$, equation (5) can be re-written in the following simpler form [29,46].

$$\Pr_{eff}\frac{\partial\tau(y,t)}{\partial t}=\frac{\partial^2\tau(y,t)}{\partial y^2};\ y,\ t\ >0, \tag{11}$$

where $\Pr_{eff}=\frac{\Pr}{1+R_c}$, $\Pr=\frac{\mu c_p}{k}$ and $R_c=\frac{16}{3}\frac{\sigma}{kk_R}\tau_\infty^3$.
Employing the following dimensionless quantities

$$y^*=\frac{F_o}{\nu}y,\ t^*=\frac{F_o{}^2}{\nu}t,\ F^*=\frac{F}{F_o},\ \tau^*=\frac{\tau-\tau_\infty}{\tau_w},\ C^*=\frac{C-C_\infty}{C_w-C_\infty},\ \beta^*=\frac{\nu}{F_o{}^2}\beta,\ K^*=\left(\frac{\nu}{F_o}\right)^2\frac{1}{K} \\ R^*=\frac{\nu}{F_o{}^2}R,\ f^*(t^*)=f\left(\frac{\nu}{F_o{}^2}t^*\right),\ g^*(t^*)=g\left(\frac{\nu}{F_o{}^2}t^*\right),\ \lambda^*=\frac{F_o{}^2}{\nu}\lambda,\ S^*=\frac{S}{\rho F_o{}^2} \tag{12}$$

Into (2), (4)–(9), (11) and dropping out the star notation, our problem transforms into following dimensionless PDEs

$$\left(1+\lambda\frac{\partial}{\partial t}\right)S(y,t)=\frac{\partial F(y,t)}{\partial y}, \tag{13}$$

$$\left(1+\lambda\frac{\partial}{\partial t}\right)\frac{\partial F(\mathrm{y,t})}{\partial t}=\frac{\partial^2 F(\mathrm{y,t})}{\partial y^2}+\left(1+\lambda\frac{\partial}{\partial t}\right)(\tau(y,t)\cos(\gamma)+NC(y,t)\cos(\gamma)- \\ -KF(\mathrm{y,t})-M\sin^2\vartheta(\mathrm{F(y,t)}-\varepsilon f(t))), \tag{14}$$

$$\Pr_{eff}\frac{\partial\tau(y,t)}{\partial t}=\frac{\partial^2\tau(y,t)}{\partial y^2}, \tag{15}$$

$$\frac{\partial C(y,t)}{\partial t}=\frac{1}{Sc}\frac{\partial^2 C(y,t)}{\partial y^2}-C_R C(y,t),\text{for } y,\ t>0 \tag{16}$$

Subject to the boundary and initial conditions

$$F(0,t)=g(t),\ \tau(0,t)=f(t),\ C(0,t)=1;\ t>0, \tag{17}$$

$$F(y,t)<\infty,\ \tau(y,t),\ C(y,t)\rightarrow 0\cdot \mathrm{as}\cdot y\rightarrow\infty, \tag{18}$$

$$F(y,0)=0,\ S(y,0)=0,\ \tau(y,0)=0,\ C(y,0)=0;\ y\geq 0, \tag{19}$$

where $N=\frac{\beta_C(C_w-C_\infty)}{\beta_\tau\tau_w}$,$M=\frac{\sigma B^2}{\rho}\frac{\nu}{F_0^2}$, and $Sc=\frac{\nu}{D_m}$.

3. Solution of the problem

It is important to mention that here our concern to find the velocity of fluid and shear stress. But, it could not be done unless we have the expressions for the temperature and concentration. In order to obtain them, we adopt the standard Laplace transform method to solve (15)-(19).

3.1. Calculation of temperature field

Now, applying Laplace transforms to (15), using the corresponding initial conditions, we find that

$$\frac{\partial^2\tilde{\tau}(y,q)}{\partial y^2}-\mathrm{Pr}_{eff}q\tilde{\tau}(y,q)=0, \tag{20}$$

With the boundary conditions

$$\tilde{\tau}(0,q)=\tilde{g}(q)\cdot\mathrm{and}\cdot\tilde{\tau}(y,q)=0\cdot\mathrm{as}\cdot y\rightarrow\infty. \tag{21}$$

The solution of the differential equation (20) along with the boundary conditions (21) is

$$\tilde{\tau}(y,q)=\tilde{f}(q)e^{-y\sqrt{\mathrm{Pr}_{eff}q}}. \tag{22}$$

Applying the inverse Laplace transform and using relation (A-1) from Appendix, the temperature field can be presented as

$$\tau(y,t)=\frac{y\sqrt{\mathrm{Pr}_{eff}}}{2\sqrt{\pi}}\int_0^t f(t-s)\frac{e^{-\left(\frac{y^2\mathrm{Pr}_{eff}}{4s}\right)}}{s^{3/2}}ds. \tag{23}$$

Moreover, the rate of heat transfer can be determined from Nusselt number (Nu), defined as

$$Nu=-\left.\frac{\partial\tau(y,t)}{\partial y}\right|_{y=0} \tag{24}$$

Using (23) in (24), we get

$$Nu=\frac{\sqrt{\mathrm{Pr}_{eff}}}{2\sqrt{\pi}}\int_0^t\frac{f(t-s)}{s^{3/2}}ds \tag{25}$$

3.2. Calculation of concentration field

Applying Laplace transform to (16), and using the corresponding initial conditions, we get

$$\frac{\partial^2\tilde{C}(y,q)}{\partial y^2}-(q+C_R)\tilde{C}(y,q)=0, \tag{26}$$

with the boundary conditions

$$\tilde{C}(0,q)=\frac{1}{q}\cdot\mathrm{and}\cdot\tilde{C}(y,q)=0\cdot\mathrm{as}\cdot y\rightarrow\infty. \tag{27}$$

The solution of Eq. (26) with the boundary conditions (27) is

$$\tilde{C}(y,q)=\frac{1}{q}e^{-y\sqrt{Sc(q+C_R)}}. \tag{28}$$

Applying the inverse Laplace transform and using relation (A-1) from Appendix, the concentration field can be presented as

$$C(y,t)=\frac{1}{2}\left[e^{-y\sqrt{C_RSc}}erfc\left(\frac{y\sqrt{Sc}}{2\sqrt{t}}-\sqrt{C_Rt}\right)+e^{y\sqrt{C_RSc}}erfc\left(\frac{y\sqrt{Sc}}{2\sqrt{t}}+\sqrt{C_Rt}\right)\right]. \tag{29}$$

The mass transfer rate known as Sherwood number(Sh) is defined as

$$Sh=-\frac{\partial C(y,t)}{\partial y}\bigg|_{y=0}. \tag{30}$$

Using (29) in (30), we get

$$Sh=\sqrt{Sc}\left(\frac{e^{-C_R t}}{\sqrt{\pi}}+\frac{1}{\sqrt{C_R}}erf\left(\sqrt{C_R t}\right)\right). \tag{31}$$

3.3. Calculation of velocity field

Applying the Laplace transform to Eq. (14) and using the $(19)_1$, we get

$$\begin{aligned}(q+\lambda q^2)\widetilde{F}(y,q)&=\frac{\partial^2\widetilde{F}(y,q)}{\partial y^2}+(1+\lambda q)\left(\widetilde{\tau}\left(y,q\right)\cos(\gamma)+N\widetilde{C}\left(y,q\right)\cos(\gamma)-\right.\\&\left.-K\widetilde{F}(y,q)-M\sin^2\vartheta\left(\widetilde{F}(y,q)-\varepsilon\widetilde{g}\left(q\right)\right)\right),\end{aligned} \tag{32}$$

with the boundary conditions

$$\widetilde{F}(0,q)=\widetilde{g}(q),\ \widetilde{F}(y,q)<\infty \ \text{as}\ y\to\infty, \tag{33}$$

where, $\widetilde{F}(y,q)=L\{f(y,t)\}$and $\widetilde{g}(q)=L\{g(t)\}$. Introducing Eqs. (22) and (28) into (32), it yields

$$\begin{aligned}&\frac{\partial^2\widetilde{F}(y,q)}{\partial y^2}-\left(\lambda q^2+(1+\lambda H)q+H\right)\widetilde{F}(y,q)=\\&=-(1+\lambda q)\left(\varepsilon M\,\widetilde{g}(q)\sin^2\vartheta+\widetilde{f}(q)\cos(\gamma)e^{-y\sqrt{\Pr_{eff}\,q}}+N\frac{1}{q}\cos(\gamma)e^{-y\sqrt{Sc(q+C_R)}}\right),\end{aligned} \tag{34}$$

where.$H=K+M\sin^2\vartheta$.

The solution of the differential equation (34) with the boundary conditions (33), is

$$\begin{aligned}\widetilde{F}\left(y,q\right)&=\widetilde{g}\left(q\right)e^{-y\sqrt{\lambda q^2+(1+\lambda H)q+H}}+\frac{\varepsilon M\sin^2\vartheta(1+\lambda q)\widetilde{g}(q)}{\lambda q^2(1+\lambda H)q+H}\left(1-e^{-y\sqrt{\lambda q^2+(1+\lambda H)q+H}}\right)+\\&+\frac{(1+\lambda q)\widetilde{f}(q)}{\left(\lambda q^2+\left(1-\Pr_{eff}+\lambda H\right)q+H\right)}\cos(\gamma)\left(e^{-y\sqrt{\Pr_{eff}q}}-e^{-y\sqrt{\lambda q^2+(1+\lambda H)q+H}}\right)+\\&+\frac{N}{q(\lambda q^2+\left(1-Sc+\lambda H\right)q+H-Sc\,\widetilde{g}(q))}\cos(\gamma)\left(e^{-y\sqrt{Sc(q+C_R)}}-e^{-y\sqrt{\lambda q^2+(1+\lambda H)q+H}}\right).\end{aligned} \tag{35}$$

Applying the inverse Laplace transform and using (A-1) and (A-2) from Appendix, the velocity field can be presented as

$$F(y,t)=F_m(y,t)+F_T(y,t)+F_C(y,t), \tag{36}$$

where

$$\begin{aligned}F_m(y,t)&=\int_0^t\psi(y,s;\lambda,H)g(t-s)ds+\\+\varepsilon M\sin^2\vartheta\int_0^t e^{-Hs}g(t-s)ds&-\varepsilon M\sin^2\vartheta\int_0^t\int_0^s g(t-s)e^{-Hu}\psi(y,s-u;\lambda,H)duds,\end{aligned} \tag{37}$$

$$\begin{aligned}&F_\tau(y,t)=\\&\frac{(1+\Pr_{eff}-\lambda H)\cos(\gamma)}{\sqrt{(1-\Pr_{eff})^2-\lambda H(2(1+\Pr_{eff})-\lambda H)}}\int_0^t\int_0^s f(t-s)e^{-\left(\frac{1-\Pr_{eff}+\lambda H}{2\lambda}\right)u}ch(b_1u)\left(\frac{y\sqrt{\Pr_{eff}}}{2\sqrt{\pi}(s-u)^{3/2}}e^{-\frac{y^2\Pr_{eff}}{4(s-u)}}-\psi(y,s-u;\lambda,H)\right)duds+\\&+\int_0^t\int_0^s f(t-s)e^{-\left(\frac{1-\Pr_{eff}+\lambda H}{2\lambda}\right)u}sh(b_1u)\left(\frac{y\sqrt{\Pr_{eff}}}{2\sqrt{\pi}(s-u)^{3/2}}e^{-\frac{y^2\Pr_{eff}}{4(s-u)}}-\psi(y,s-u;\lambda,H)\right)duds,\end{aligned} \tag{38}$$

$$F_C\left(y,t\right)=\frac{N\cos(\gamma)}{H-ScC_R}\left(\varphi\left(y\sqrt{Sc},t;C_R,0\right)-\int_0^t\psi(y,s;\lambda,H)ds+\right.$$
$$\left.+\int_0^t e^{-\frac{1-Sc+\lambda H}{2\lambda}}\left(\frac{y\sqrt{Sc}\,e^{-\frac{Scy^2+4C_R(t-s)^2}{4(t-s)}}}{2\sqrt{\pi}(t-s)^{3/2}}-\psi(y,t-s;\lambda,H)\right)\left(\frac{(\lambda(H-2ScC_R)-(1-Sc))sh(b_2s)-ch(b_2s)}{\sqrt{(1-Sc)^2+\lambda(H(\lambda H-2Sc-2)+4ScC_R)}}\right)ds\right) \tag{39}$$

Denotes the mechanical, thermal and concentration components, respectively. In the above expressions

$$b_1=\frac{\sqrt{\left(1-\Pr_{eff}+\lambda H\right)^2-4\lambda H}}{2\lambda},b_2=\frac{\sqrt{(1-Sc+\lambda H)^2-4\lambda(H-ScC_R)}}{2\lambda}.$$

Moreover, the functions $\varphi(y,t;a,b)$ and $\psi(y,t;\lambda,H)$are defined in Appendix (A-2) and (A-9), respectively.
It can easily verify that $F(y,t)$, given by Eq. (36), satisfies the imposed boundary and initial conditions.
Further, as $y\to\infty$, we have

$$\lim_{y\to\infty}F(y,t)=\begin{cases}0 & if\ \varepsilon=0\\ M\sin^2\vartheta\int_0^t e^{-Hs}g(t-s)ds & if\ \varepsilon=1.\end{cases} \tag{40}$$

Finally, for the case MFFRP, far away from the plate the fluid does not remain at rest.

Certainly, by customizing to $f(\cdot)$ and $g(\cdot)$ suitable forms, we can recover the exact solutions for any motion with technical relevance of this type that is discussed in section 4.

3.4. Calculation of shear stress

Taking Laplace transform of (13) and making use of condition $(19)_2$, we obtain

$$(1+\lambda q)\widetilde{S}(y,q)=\frac{\partial\widetilde{F}(y,q)}{\partial y}, \tag{41}$$

$$\widetilde{S}(y,q)=\frac{1}{1+\lambda q}\frac{\partial\widetilde{F}(y,q)}{\partial y}. \tag{42}$$

Plugging Eq. (35) in the last expression, we get

$$\begin{aligned}\widetilde{S}(y,q)=&-\frac{\sqrt{\lambda q^2+(1+\lambda H)q+H}}{1+\lambda q}e^{-y\sqrt{\lambda q^2+(1+\lambda H)q+H}}\widetilde{g}(q)+\frac{\varepsilon M\widetilde{g}(q)e^{-y\sqrt{\lambda q^2(1+\lambda H)q+H}}\sin^2\vartheta}{\sqrt{\lambda q^2+(1+\lambda H)q+H}}+\\&+\frac{\widetilde{f}(q)\left(\sqrt{\lambda q^2+(1+\lambda H)q+H}\,e^{-y\sqrt{\lambda q^2+(1+\lambda H)q+H}}-\sqrt{\Pr_{eff}q}\,e^{-y\sqrt{\Pr_{eff}q}}\right)}{\left(\lambda q^2+\left(1-\Pr_{eff}+\lambda H\right)q+H\right)}\cos(\gamma)+\\&+\frac{N\left(\sqrt{\lambda q^2+(1+\lambda H)q+H}\,e^{-y\sqrt{\lambda q^2+(1+\lambda H)q+H}}-\sqrt{Sc(q+C_R)}\,e^{-y\sqrt{Sc(q+C_R)}}\right)}{q(1+\lambda q)(\lambda q^2+(1-Sc+\lambda H)q+H-ScC_R)}\cos(\gamma).\end{aligned} \tag{43}$$

As the above expression represents the shear stress solutions in terms of the Laplace transform parameter$q$, it is therefore inverted back to the original time domain with the help of a numerical Laplace inversion called Stehfest's algorithm for numerical inversion of Laplace transform [48]. Employing this algorithm, we have

$$S(y,t)=\frac{\ln 2}{t}\sum_{i=1}^{2p}(-1)^{i+p}\sum_{n=\left[\frac{i+1}{2}\right]}^{\min(i,p)}\frac{n^p(2n)!}{(p-n)!n!(n-1)!(i-n)!(2n-i)!}\widetilde{\tau}\left(y,\frac{\ln 2}{q}\right), \tag{44}$$

where $p$is a positive integer and $[\cdot]$ denotes the positive part of the real number.

Now, in the next section, with the aim to get some physical understanding of the obtained results, we shall consider the dynamics of fluid under the influence of different modes of heating of plate as well as general the motion of the plate.

4. Different cases regarding temperature distribution and the motion of the plate

Observed that, heat and mass transfer can influence the fluid motion, so logically it is required to know that if their influence is prominent or it can be ignored in some motions with desirable engineering applications.

Now, we will discuss the solutions corresponding to different modes of heating of the plate.

4.1. Case-I: $f(t) = H(t)$ (constant heating of the plate)

Substituting $f(t) = H(t)$ in (38), we get

$$
\begin{aligned}
F_{\tau_{con}}(y,t) = & \frac{1}{H}\left(erfc\left(\frac{y}{2\sqrt{t}}\right) - \int_0^t \psi(y,s;\lambda,H)ds\right)\cos(\gamma) - \\
& -\frac{1}{H}\cos(\gamma)\int_0^t e^{-\left(\frac{1-\mathrm{Pr}_{eff}+\lambda H}{2\lambda}\right)u} ch(b_1 s)\left(erfc\left(\frac{y}{2\sqrt{t-s}}\right) - \psi(y,t-s;\lambda,H)\right)ds + \\
& + \frac{(\lambda H - (1-\mathrm{Pr}_{eff}))\cos(\gamma)}{H\sqrt{(1-\mathrm{Pr}_{eff})^2 + \lambda(\lambda H(H - 2(1+\mathrm{Pr}_{eff})))}}\int_0^t e^{-\left(\frac{1-\mathrm{Pr}_{eff}+\lambda H}{2\lambda}\right)u} sh(b_1 s)\left(erfc\left(\frac{y}{2\sqrt{t-s}}\right) - \psi(y,t-s;\lambda,H)\right)ds.
\end{aligned} \tag{45}
$$

Moreover, in this case by substituting $f(t) = H(t)$ in (25) gives

$$
Nu = \sqrt{\frac{\mathrm{Pr}_{eff}}{\pi t}}. \tag{46}
$$

4.2. Case-II: $f(t) = H(t)(1 - \alpha e^{-\beta t})$ (exponential heating of the plate)

Substituting $f(t) = H(t)(1 - \alpha e^{-\beta t})$ where $0 < \beta < \alpha < 1$, in (38), we get

$$
\begin{aligned}
F_{\tau\,\exp}(y,t) = & \frac{1}{H}\left(erfc\left(\frac{y}{2\sqrt{t}}\right) - \int_0^t \psi(y,s;\lambda,H)ds\right)\cos(\gamma) + \\
& + \frac{\alpha(\beta\lambda - 1)\cos(\gamma)}{\lambda\beta^2 - (1-\mathrm{Pr}_{eff}+\lambda H)\beta + H}\left(\varphi\left(y\sqrt{\mathrm{Pr}_{eff}}, t; 0, -\beta\right) - \int_0^t e^{-\beta u}\psi(y,t-s;\lambda,H)ds\right) + \\
& + \frac{(1-\mathrm{Pr}_{eff})\beta - (1+\alpha)H - \lambda\beta(\beta-(1-\alpha)H)}{H(\lambda\beta(\beta-H) - (1-\mathrm{Pr}_{eff})\beta + H)}\cos(\gamma)\int_0^t e^{-\left(\frac{1-\mathrm{Pr}_{eff}+\lambda H}{2\lambda}\right)u} ch(b_1 s)\left(erfc\left(\frac{y}{2\sqrt{t-s}}\right) - \psi(y,t-s;\lambda,H)\right)ds + \\
& + A\cos(\gamma)\int_0^t e^{-\left(\frac{1-\mathrm{Pr}_{eff}+\lambda H}{2\lambda}\right)u} sh(b_1 s)\left(erfc\left(\frac{y}{2\sqrt{t-s}}\right) - \psi(y,t-s;\lambda,H)\right)ds,
\end{aligned} \tag{47}
$$

where

$$
\begin{aligned}
A = & \frac{2\lambda(1-\mathrm{Pr}_{eff})\left((\alpha-1)H + \beta(1-\mathrm{Pr}_{eff}) + \lambda\beta((H-\beta)(1-\mathrm{Pr}_{eff}) - H\alpha)\right)}{H(H - (1-\mathrm{Pr}_{eff})\beta - \lambda\beta(H-\beta))\sqrt{(1-\mathrm{Pr}_{eff}+\lambda H)^2 - 4\lambda H}} - \\
& - \frac{1-\mathrm{Pr}_{eff}+\lambda H}{\sqrt{(1-\mathrm{Pr}_{eff}+\lambda H)^2 - 4\lambda H}}\frac{\lambda}{H}\frac{(1-\mathrm{Pr}_{eff})\beta - (1+\alpha)H - \lambda\beta(\beta-(1-\alpha)H)}{\lambda\beta(\beta-H) - (1-\mathrm{Pr}_{eff})\beta + H}.
\end{aligned}
$$

Again, customizing $f(t) = H(t)(1 - \alpha e^{-\beta t})$ in (25) yields

$$
Nu = (1-\alpha)\sqrt{\frac{\mathrm{Pr}_{eff}}{\pi t}} + \alpha e^{-\beta t}\sqrt{\beta \mathrm{Pr}_{eff}}\, erf\left(i\sqrt{\beta t}\right). \tag{48}
$$

Now, we will discuss the solutions corresponding to motions due to a variably accelerating plate (when $\delta > 0$) and oscillating motion of the plate.

4.3. Case-III: $g(t) = H(t)t^{\delta}$ (variably accelerating plate)

Now, substituting $g(t) = H(t)t^{\delta}$, with $\delta > 0$, into equation (37), we get

$$
\begin{aligned}
F_m(y,t) = & \int_0^t \psi(y,s;\lambda,H)(t-s)^{\delta}ds + \varepsilon M\sin^2\vartheta\int_0^t e^{-Hs}(t-s)^{\delta}ds - \\
& -\varepsilon M\int_0^t\int_0^s (t-s)^{\delta}e^{-Hu}\psi(y,s-u;\lambda,H)duds,
\end{aligned} \tag{49}
$$

which represents motions due to a slowly, constantly or highly accelerating plate.

Moreover, the case relating to $\delta = 0$, i.e. when plate moves with constant velocity

$$F_{0m}(y,t) = \int_0^t \psi(y,s;\lambda,H)ds + \varepsilon\left(1-e^{-Ht}\right) - \varepsilon M\sin^2\vartheta \int_0^t\int_0^s e^{-Hu}\psi(y,s-u;\lambda,H)duds. \tag{50}$$

Further, by taking limit $\lambda \to 0, \gamma = 0, \vartheta = \frac{\pi}{2}$ and $K = 0$for Eq. (48), yields

$$F_m(y,t) = \frac{y}{2\sqrt{\pi}} \int_0^t \frac{(t-s)^\delta}{s\sqrt{s}} \exp\left(-\frac{y^2}{4s} - Hs\right)ds + \varepsilon M\sin^2\vartheta \int_0^t (t-s)^\delta e^{-Hs} erf\left(\frac{y}{2\sqrt{s}}\right)ds, \tag{51}$$

The solutions for free convection flows of viscous fluid on a moving vertical plate [18].

4.4. Case-IV:$g(t) = H(t)\cos(\omega t)$ or $H(t)\sin(\omega t)$ (oscillating plate)

Putting $g(t) = H(t)\cos(\omega t)$ or $H(t)\sin(\omega t)$into Eq. (37), we obtain

$$\begin{aligned} F_{cm}(y,t) = & \int_0^t \psi(y,s;\lambda,H)\cos(\omega(t-s))ds + \varepsilon M\left(\frac{He^{-Ht}}{H^2+\omega^2} + \frac{\cos(\omega t+\theta)}{\sqrt{H^2+\omega^2}}\right) - \\ & -\varepsilon M \int_0^t \left(\frac{He^{-Hs}}{H^2+\omega^2} + \frac{\cos(\omega s+\theta)}{\sqrt{H^2+\omega^2}}\right)\psi(y,t-s;\lambda,H)ds, \end{aligned} \tag{52}$$

$$\begin{aligned} F_{sm}(y,t) = & \int_0^t \psi(y,s;\lambda,H)\sin[\omega(t-s)]ds + \varepsilon M\sin^2\vartheta\left(\frac{\omega e^{-Ht}}{H^2+\omega^2} + \frac{\sin(\omega t-\theta)}{\sqrt{H^2+\omega^2}}\right) - \\ & -\varepsilon M\sin^2\vartheta \int_0^t \left(\frac{\omega e^{-Hs}}{H^2+\omega^2} + \frac{\sin(\omega s-\theta)}{\sqrt{H^2+\omega^2}}\right)\psi(y,t-s;\lambda,H)ds. \end{aligned} \tag{53}$$

It is important to note that, the dimensionless velocities$F_{cm}(y,t)$ and $F_{sm}(y,t)$(as represented by Eqs. (52) and (53)) represents the motion of fluid sometime after its initiation. After sometime, when the transients departs, Eqs. (52) and (53) become

$$\begin{aligned} F_{cmp}(y,t) = & \int_0^\infty \psi(y,s;\lambda,H)\cos(\omega(t-s))ds + \frac{\varepsilon M\sin^2\vartheta}{\sqrt{H^2+\omega^2}}\cos(\omega t+\theta) - \\ & -\frac{\varepsilon M\sin^2\vartheta}{\sqrt{H^2+\omega^2}} \int_0^\infty \cos(\omega s+\theta)\,\psi(y,t-s;\lambda,H)ds, \end{aligned} \tag{54}$$

$$\begin{aligned} F_{smp}(y,t) = & \int_0^\infty \psi(y,s;\lambda,H)\sin[\omega(t-s)]ds + \frac{\varepsilon M\sin^2\vartheta}{\sqrt{H^2+\omega^2}}\sin(\omega t-\theta) - \\ & -\frac{\varepsilon M\sin^2\vartheta}{\sqrt{H^2+\omega^2}} \int_0^\infty \sin(\omega s-\theta)\,\psi(y,t-s;\lambda,H)ds, \end{aligned} \tag{55}$$

The steady-state solutions.

Moreover, it is easy to verify that these solutions satisfy the boundary conditions and governing equation (14) in absence of thermal effects and concentration. As a result, in the absence of these effects, after a certain characteristic time fluid flow according to Eqs. (54) and (55). Taking the limit $y \to \infty$ on Eqs. (54) and (55), we get

$$F_{cmp}(\infty,t) = \begin{cases} 0 & if\ \varepsilon = 0 \\ \dfrac{M\sin^2\vartheta}{\sqrt{H^2+\omega^2}}\cos(\omega t-\theta) & if\ \varepsilon = 1, \end{cases} \tag{56}$$

Respectively

$$F_{smp}(\infty,t) = \begin{cases} 0 & if\ \varepsilon = 0 \\ \dfrac{M\sin^2\vartheta}{\sqrt{H^2+\omega^2}}\sin(\omega t-\phi) & if\ \varepsilon = 1. \end{cases} \tag{57}$$

Now, for analogy, if we take $g(t) = H(t)\cos(\omega t)$ or $g(t) = H(t)\sin(\omega t)$ into Eq. (40). The related results

$$F_c(\infty,t) = \begin{cases} 0 \quad if\ \varepsilon = 0 \\ -\dfrac{M^2 \sin^4 \vartheta}{H^2+\omega^2} e^{-Ht} + \dfrac{M \sin^2 \vartheta}{\sqrt{H^2+\omega^2}} \cos(\omega t - \theta)\ if\ \varepsilon = 1, \end{cases} \tag{58}$$

$$F_s(\infty,t) = \begin{cases} 0 \quad if\ \varepsilon = 0 \\ \dfrac{M\omega \sin^2 \vartheta}{H^2+\omega^2} e^{-Mt} + \dfrac{M \sin^2 \vartheta}{\sqrt{H^2+\omega^2}} \sin(\omega t - \theta) \quad if\ \varepsilon = 1, \end{cases} \tag{59}$$

Agree with those from Eqs. (55) and (56). Eqs. (58) and (59) also involve the transient parts of velocity.

5. Results validation

In order to check the validation of our results, by taking $K = 0, \lambda = 0, \vartheta = \frac{\pi}{2}, \gamma = 0$ and $f(t) = H(t)(1 - \alpha e^{-\beta t})$in Eqs. (37)–(39) we get the corresponding results of Shah et al. [18, Eqs. (27)–(29)] for the case of viscous fluid. Moreover, for $g(t) = H(t)$ and $\lambda = 0, \vartheta = \frac{\pi}{2}$ and $\gamma = 0$,in (37) and using relations (A-3) and (A-4) from the Appendix. As it is expected, the obtained results are similar to those reported by Narahari and Debnath [16, Eqs. (11a) with $a_o = 0$] and Tokis [47, Eq. (12)] when there are no thermal, porous and concentration effects.

Again for $\lambda = 0, K = 0, \vartheta = \frac{\pi}{2}, \gamma = 0$,$f(t) = H(t)(1 - \alpha e^{-\beta t})$and $g(t) = H(t)\sin(\omega t)orH(t)\cos(\omega t)$, Eq. (37) yields the corresponding results for the case of viscous fluid [18], as follow

$$F_{sm}(y,t) = \frac{y}{2\sqrt{\pi}} \int_0^t \frac{\sin(\omega(t-s))}{s\sqrt{s}} e^{-\left(\frac{y^2}{4s}+Ms\right)} ds + \varepsilon M \int_0^t \sin(\omega(t-s)) e^{-Ms} erf\left(\frac{y}{2\sqrt{s}}\right) ds, \tag{60}$$

$$F_{cm}(y,t) = \frac{y}{2\sqrt{\pi}} \int_0^t \frac{\cos(\omega(t-s))}{s\sqrt{s}} e^{-\left(\frac{y^2}{4s}+Ms\right)} ds + \varepsilon M \int_0^t \cos(\omega(t-s)) e^{-Ms} erf\left(\frac{y}{2\sqrt{s}}\right) ds. \tag{61}$$

6. Numerical results and discussion

In this article, the MHD free convection flow of Maxwell fluid on a porous layered inclined plate is investigated. The problem is simulated as the natural convection for oscillating and general emotions of an inclined plate embedded in a porous medium in the presence of slanted external magnetic field that is either fixed or moves along with the plate. Heat transfer analysis is carried out by considering constant concentration, first order chemical reaction and thermal conductivity as a general function of time. The non-dimensional partial differential equations are solved by Laplace transform method. Mechanical, thermal and concentration effects on the fluid motion are independently taken into account. In order to get the physical understanding of obtained results, several cases of theoretical interest with engineering applications I have been taken and some already established results in the existing literature have been recovered as limiting case. Moreover, the influence of essential parameters and variables N,Sc,C_R and λ especially the inclination of the plate (with the vertical) and slanted magnetic field on the motion of the fluid is graphically analyzed and discussed

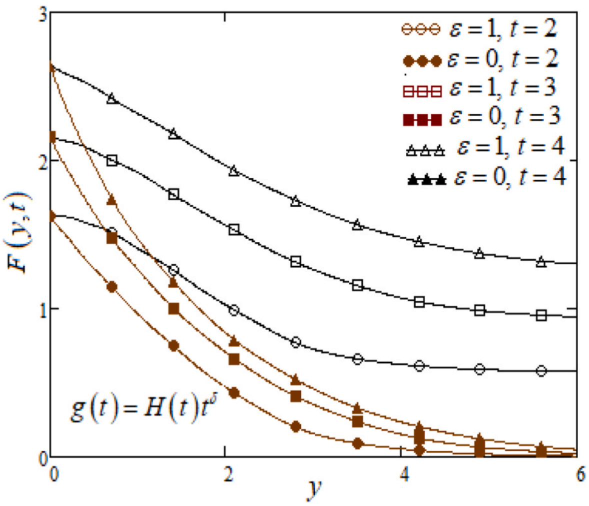

Fig. 1. Plots of $F(y,t)$iversusi y for $N = 2.5$,$\mathrm{Pr}_{eff} = 4.5$,$Sc = 0.8$,$\lambda = 0.5$,$C_R = 0.7$,$K = 1$,$\vartheta = \frac{\pi}{6}$,$\gamma = \frac{\pi}{6}$, and different values of t.

for a slowly accelerating motion of the plate.

Fig. 1 is prepared to show the plot of the velocity $F(y,t)$ versus y at different times. As reported, the profiles corresponding to MFSRP are considerably larger in comparison to the case of MFSRF. Moreover, there is a smooth decrease in velocity from certain maximum value on the boundary to an asymptotical value as y increases. Further, as recorded from these diagrams that, the asymptotic values of velocities are non-zero as y goes to infinity for the case of MFSRP.

Fig. 2 presents the influence of buoyancy force parameter on the velocity of the fluid. Here, $F(y,t)$ is plotted versus y at $t=2$ for several values of N. It is observed that velocity of fluid increases for increasing values of N. Because, for $N>0$, the buoyancy force due to the species diffusion supports the thermal buoyancy force and as a result velocity of the fluid increases for increasing values of N. But, for $N<0$,species diffusion opposes the thermal buoyancy forces and hence resists the flow of fluid. Moreover, as buoyancy forces ratio parameter calibrates the relative contribution of the mass flux on the free convection flow, so we can say that increase in mass fluxion the free convection flow increases the velocity of the fluid.

The influence of the chemical reaction parameter C_R on velocity of fluid is recorded in Fig. 3. From this figure, it is noticed that the velocity decreases corresponding to the increasing value of chemical reaction parameter. Increase in the chemical reaction parameter suppresses the concentration of the fluid and concentration distribution decreases throughout the fluid flow field ultimately decreases the concentration buoyancy effects and hence, velocity of the fluid decreases. Furthermore, it is reported that the velocity profiles are higher in the case when magnetic field is fixed relative to the plate.

Moreover, the contributions of the three components of velocity (mechanical, thermal and concentration) on the fluid motion are plotted in Fig. 4 both for MFSRF and MFSRP. It is evident from these figures that each component contributes and has an appreciable influence on the fluid velocity and hence, cannot be neglected. As reported from Figs. 5 and 6, the velocity of the fluid decreases with the increase in inclination of the plate with the vertical as well as the parameter of porosity. Moreover, velocity of the fluid decreases with the increase of slant angle $\vartheta \in \left[0,\frac{\pi}{2}\right]$ of the magnetic field with the plate. For increasing values of $\vartheta \in \left[0,\frac{\pi}{2}\right]$, the magnetic term $M=\frac{\sigma B^2 \sin^2\vartheta}{\rho}$ is getting stronger and its effects on an electrically conducting fluid give rise to a Lorentz force, that has the tendency to slow down the motion of the fluid and increases its boundary layer. This result qualitatively agrees with the expectations, since magnetic field exerts retarding force on the free convection flow. So, we can control the strength of the magnetic term not only by magnetic field strength parameter B but also by the slant angle ϑ to get the desired controls. It is reported from Fig. 7 that heat transfer rate is an increasing function of effective Prandtl number but decays with time. Moreover, in Fig. 8, we have plotted Sh versus t for different values of C_R. It is observed that the rate of mass transfer increases with the increasing values of chemical reaction parameter as well as the transport parameter. Because, increase in the values of chemical reaction parameter implies more interaction of species concentration with momentum boundary layer that results in as an increase in the mass transfer rate. In all of the figures (Figs. 1–8) we have fixed. $\alpha=0.70,\ \beta=0.10, B=0.6$.

7. Conclusions

Magneto-free-convection flows of Maxwell fluid on a porous layered inclined plate have been investigated. The problem is modeled as natural convection for general motions of an inclined plate moving in a magnetized medium with a slanted external magnetic field that is either stationary or moving in the same direction as the plate's plane. Constant concentration, first order chemical reaction, and thermal conductivity as a general function of time are used in heat transfer analysis. On the velocity of the fluid, the effects of varied plate angles with the wall, as well as the slanted angle of the magnetic field with the plate, are examined. The velocity of the plate and

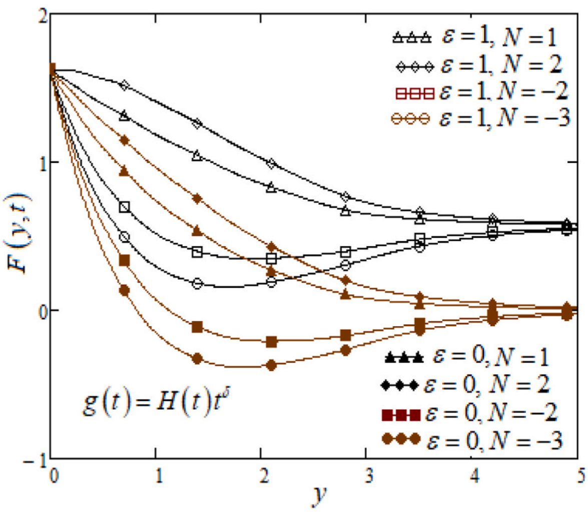

Fig. 2. Plots of $F(y,t)$ versusi y at $t=2$ for $\Pr_{eff}=4.5, Sc=0.8, \lambda=0.5, C_R=0.7, K=1, \vartheta=\frac{\pi}{6}, \gamma=\frac{\pi}{6}$, and different values of N.

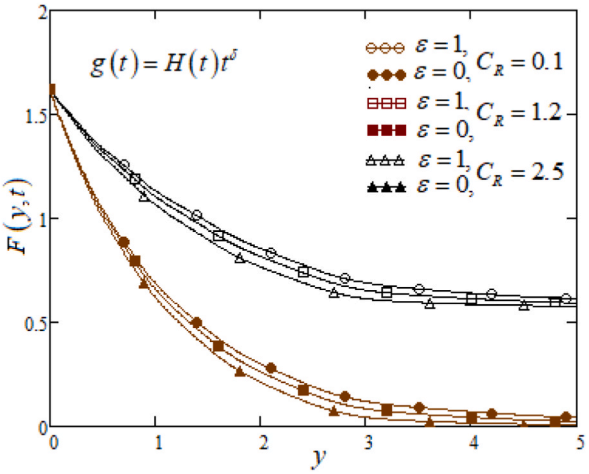

Fig. 3. Plots of $F(y,t)$ versusyat $t = 2.5$ for $\text{Pr}_{eff} = 4.5, N = 2.5, \lambda = 0.5, Sc = 0.8, K = 1, \vartheta = \frac{\pi}{6}, \gamma = \frac{\pi}{6}$, and different values of C_R.

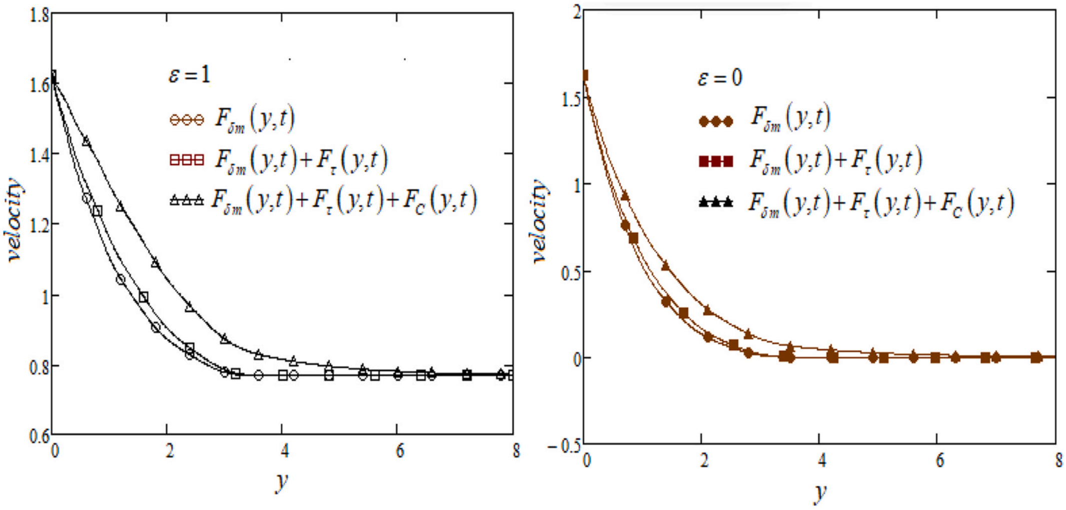

Fig. 4. Behaviour of velocities $F_{\delta m}(y,t), F_{\delta m}(y,t) + F_C(y,t)$ and $F_{\delta m}(y,t) + F_\tau(y,t) + F_C(y,t)$ versusy at $t = 2$ for $\text{Pr}_{eff} = 4.5, N = 2.5, C_R = 0.7, Sc = 0.8, K = 1, \vartheta = \frac{\pi}{6}, \gamma = \frac{\pi}{6}$, and $\lambda = 0.5$.

temperature distribution in certain circumstances are described. Furthermore, for the condition of a slowly accelerating motion and exponential heating of the plate, parametric analysis on fluid dynamics is performed using graphical simulations. The following are the key findings:

- The fluid velocity is significantly larger in the case when magnetic field is fixed relative to the plate as compared to the case when it is fixed with respect to fluid.
- Far away from the plate velocity of the fluid does not become zero if the magnetic field is fixed relative to the plate.
- Velocity of the fluid increases for increasing values of buoyancy forces ratio parameter N.
- Contributions of mechanical, thermal and concentration components of velocity are considerable and they cannot be ignored.
- The velocity of the fluid decreases with the increase in the angle of inclination of the plate with the vertical as well as the parameter of porosity.
- Mass flux increases with the increase in buoyancy ratio.
- Increase in the slant angle of the magnetic field and chemical reaction parameter retargeted motion of the fluid.
- Motion of the fluid could be controlled not only by the strength of the magnetic parameter but also by the slant angle of magnetic field.

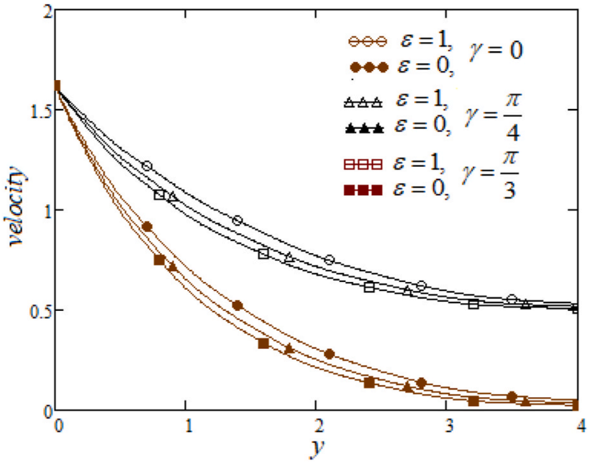

Fig. 5. Plots of $F(y,t)$versusyat $t = 1.5$ for $\mathrm{Pr}_{eff} = 4.5$,$N = 2.5$,$C_R = 0.7$,$Sc = 0.8$,$K = 1$,$\vartheta = \frac{\pi}{6}$,$\lambda = 0.5$ and different values of inclination of the plate with the vertical.

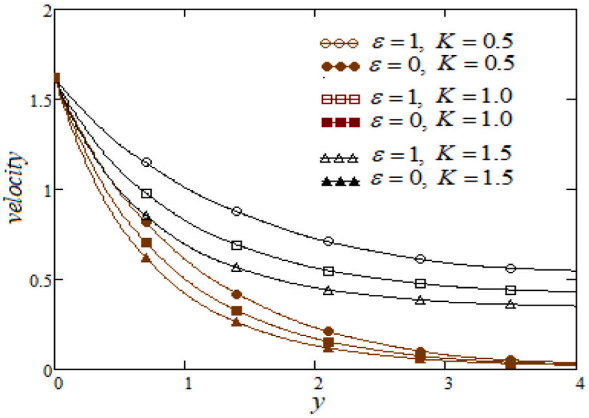

Fig. 6. Plots of $F(y,t)$versusyat $t = 1.5$ for $\mathrm{Pr}_{eff} = 4.5$,$N = 2.5$,$C_R = 0.7$,$Sc = 0.8$,$\vartheta = \frac{\pi}{6}$,$\gamma = \frac{\pi}{6}$,$\lambda = 0.5$ and different values of K.

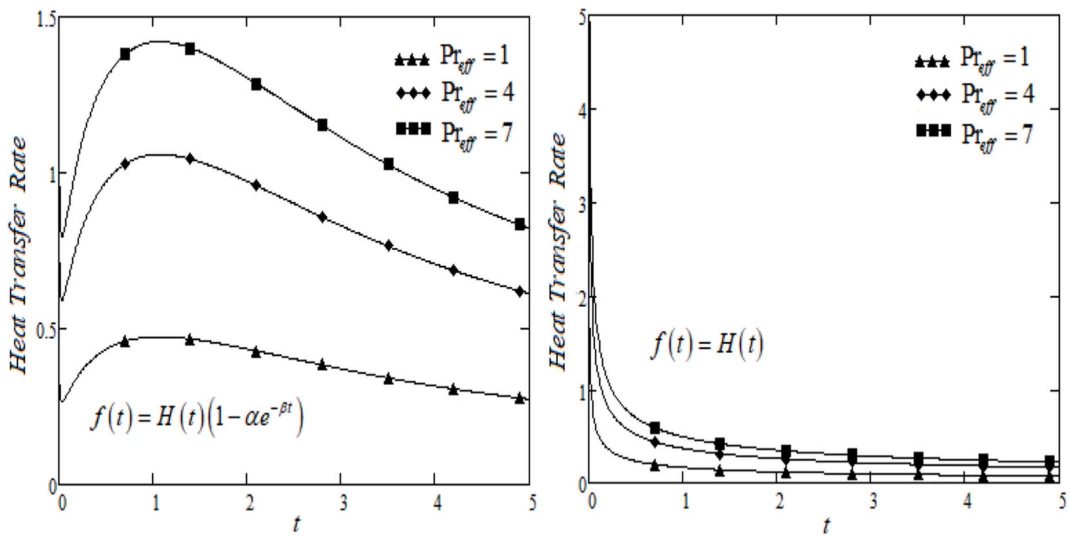

Fig. 7. Behaviour of heat transfer rate for different values of effective Prandtl number.

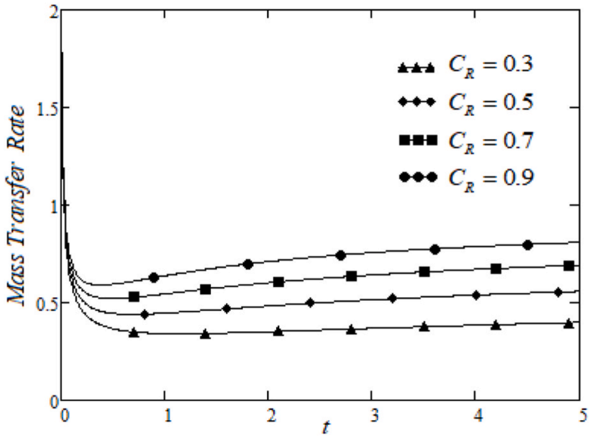

Fig. 8. Behaviour of mass transfer rate for different values of chemical reaction parameter.

Declaration of competing interest

The authors declare that they have no known competing financial interests or personal relationships that could have appeared to influence the work reported in this paper.

Acknowledgments

The work in this paper has been supported by the Polish National Science Centre under the grant OPUS 14 No. 2017/27/B/ST8/01330 and Basic Science Research Program through the National Research Foundation of Korea (NRF) funded by the Ministry of Science, ICT & Future Planning (Grant number: 2017R1A2B2006927).

Appendix A

$$L^{-1}\left\{e^{-y\sqrt{q}}\right\}=\frac{y}{2t\sqrt{\pi t}}\exp\left(-\frac{y^2}{4t}\right),\ L^{-1}\left\{\frac{e^{-y\sqrt{q}}}{q}\right\}=erfc\left(\frac{y}{2\sqrt{t}}\right),\ L^{-1}\left\{\frac{e^{-y\sqrt{q+a}}}{q-b}\right\}=\varphi(y,t;a,b). \tag{A-1}$$

$$\varphi\left(y,t;a,b\right)=\frac{e^{bt}}{2}\left[e^{-y\sqrt{a+b}}erfc\left(\frac{y}{2\sqrt{t}}-\sqrt{(a+b)t}\right)+e^{y\sqrt{a+b}}erfc\left(\frac{y}{2\sqrt{t}}+\sqrt{(a+b)t}\right)\right]. \tag{A-2}$$

$$\int_0^t\frac{1}{\sqrt{s}}\exp\left(-\frac{y^2}{4s}-as\right)ds=\frac{\sqrt{\pi}}{2\sqrt{a}}\left\{e^{-y\sqrt{a}}erfc\left(\frac{y}{2\sqrt{t}}-\sqrt{at}\right)-e^{y\sqrt{a}}erfc\left(\frac{y}{2\sqrt{t}}+\sqrt{at}\right)\right\}. \tag{A-3}$$

$$\int_0^t\frac{1}{s\sqrt{s}}\exp\left(-\frac{y^2}{4s}-as\right)ds=\frac{\sqrt{\pi}}{y}\left\{e^{-y\sqrt{a}}erfc\left(\frac{y}{2\sqrt{t}}-\sqrt{at}\right)-e^{y\sqrt{a}}erfc\left(\frac{y}{2\sqrt{t}}+\sqrt{at}\right)\right\}. \tag{A-4}$$

$$L^{-1}\{e^{-aq}\}=\delta(t-a). \tag{A-5}$$

$$f(t)*\delta(t-a)=f(t-a). \tag{A-6}$$

$$L^{-1}\left\{e^{a\left(q-\sqrt{q^2-b^2}\right)}-1\right\}=\frac{ab}{\sqrt{t^2+2at}}I_1\left(b\sqrt{t^2+2at}\right), \tag{A-7}$$

where $I_1(\cdot)$ is the modified Bessel function of first kind.

$$L^{-1}\left\{e^{-y\sqrt{(q+a)^2-b^2}}\right\}=e^{-ya}\delta(t-a)+e^{-at}\frac{by}{t^2-y^2}I_1\left(b\sqrt{t^2-y^2}\right). \tag{A-8}$$

$$\begin{aligned} &L^{-1}\left\{e^{-y\sqrt{\lambda q^2(1+\lambda M)q+M}}\right\} = \psi(y,t;\lambda,M) \\ &\psi(y,t;\lambda,M) = e^{-y\frac{1+\lambda M}{2\sqrt{\lambda}}}\delta\left(t-y\sqrt{\lambda}\right) + e^{-\frac{1+\lambda M}{2\lambda}t}\frac{1-\lambda M}{2\sqrt{\lambda}}\frac{y}{t^2-y^2\lambda}I_1\left(\frac{1-\lambda M}{2\lambda}\sqrt{t^2-y^2\lambda}\right). \end{aligned} \tag{A-9}$$

Author statement

Azhar Ali Zafar: Conceptualization; Writing – original draft; Methodology; Jan Awrejcewicz: Data curation; Investigation; Grzegorz Kudra: Formal analysis; Investigation; Nehad Ali Shah: Writing – original draft; Methodology; Resources; Writing – review & editing; Se-Jin Yook: Supervision.

References

[1] J. Hartmann, Theory of the laminar flow of an electrically conductive liquid in a homogeneous magnetic field, Fys. Med. 15 (1937) 1–27.
[2] J. Hartmann, F. Lazarus, Experimental investigations on the flow of mercury in a homogeneous magnetic field, Mat. Fys. Medd. K. Dan. Vidensk. Selsk. 15 (7) (1937) 1–46.
[3] J.T. Stuart, On the stability of viscous flow between parallel planes in the presence of a Co-planar magnetic field, Proc. Roy. Soc. of London, ser. A. 221 (1145) (1954) 189–206.
[4] R.C. Lock, Stability of the flow of an electrically conducting fluid between -parallel planes under a transverse magnetic field, Proc. Roy. Soc. of London, ser. A. 233 (1192) (1955) 105–125.
[5] V.J. Rossow, On Flow of Electrically Conducting Fluids over a Flat Plate in the Presence of a Transverse Magnetic Field, National Advisory Committee for Aeronautics, 1957. Report 1358.
[6] B. Gebhart, Y. Jaluria, R.L. Mahajan, B. Sammakia, Buoyancy Induced Flows and Transport, Hemisphere, Washington D.C., 1988.
[7] S. Nadeem, R. Mehmood, N.S. Akbar, Non-orthogonal stagnation point flow of a nano non-Newtonian fluid towards a stretching surface with heat transfer, Int. J. Heat Mass Tran. 57 (2013) 679–689.
[8] A. Ghosh, P. Sana, On hydromagnetic flow of an Oldroyd-B fluid near a pulsating plate, Acta Astronaut. 64 (2009) 272–280.
[9] M. Amkadni, A. Azzouzi, Z. Hammouch, On the exact solutions of laminar MHD flow over a stretching plate, Commun Nonlinear Sci 13 (2) (2008) 359–368.
[10] S. Gupta, D. Kumar, J. Singh, MHD mixed convective stagnation point flow and heat transfer of an incompressible nano fluid over an inclined stretching sheet with chemical reaction and radiation, Int. J. Heat Mass Tran. 118 (2019) 378–387.
[11] O. Aydin, A. Kaya, MHD mixed convection of a viscous dissipating fluid about permeable vertical flat plate, Appl. Math. Model. 33 (110) (2009) 4086–4096.
[12] B.K. Jha, C.A. Apere, Combined effect of hall and ion-slip currents on unsteady MHD Couette flows in a rotating system, J. Phys. Soc. Jpn. 79 (2010) 104–401.
[13] E.F. Elshehawey, E.M.E. Elbarbary, N.S. Elgazery, Effect of inclined magnetic field on magneto fluid flow through a porous medium between two inclined wavy porous plates (numerical study), Appl. Math. Comput. 135 (1) (2003) 85–103.
[14] R. Nandkeolyar, M. Das, MHD free convective radiative flow past a flat plate with ramped temperature in the presence of an inclined magnetic field, Comput. Appl. Math. 34 (2015) 109–123.
[15] M.F. Endalew, A. Nayak, Thermal radiation and inclined magnetic field effects on MHD flow past a linearly accelerated inclined plate in a porous medium with variable temperature, Heat Tran. Asian Res. 1 (2019) 42–61.
[16] M. Narahari, L. Debnath, Unsteady magnetohydrodynamic free convection flow past an accelerated vertical plate with constant heat flux and heat generation or absorptio, Z. Angew. Math. Mech. 93 (2013) 38–49.
[17] N.A. Shah, A.A. Zafar, S. Akhtar, General solution for MHD-free convection flow over a vertical plate with ramped wall temperature and chemical reaction, Arab J Math 7 (2018) 49–60.
[18] N.A. Shah, A.A. Zafar, C. Fetecau, A. Naseem, Effects of Exponential Heating on Double-Diffusive Free Convection Flows on a Moving Vertical Plate, 2019. Accepted for publication in Math Reports.
[19] E.M. Sparrow, R.B. Husar, Longitudinal vortices in Natural convection flow on inclined plates, J. Fluid Mech. 37 (1969) 251–255.
[20] S. Siddiqa, S. Asghar, M.A. Hossain, Natural convection flow over an inclined flat plate with internal heat generation and variable viscosity, Math. Comput. Model. 52 (2010) 1739–1751.
[21] M. Bhuvaneswari, S. Sivasankaran, Free convection flow in an inclined plate with variable thermal conductivity by scaling group transformations, AIP Conference Proceedings 1605 (2014) 440, https://doi.org/10.1063/1.4887629.
[22] E.K. Zariffeh, M. Daguenet, Laminar free convection on an inclined flat plate or a vertical cylinder with prescribed wall heat flux, Int. J. Heat Mass Tran. 24 (6) (1981) 1071–1075.
[23] A. Tumin, The Spatial stability of natural convection flow on inclined plates, J FluidEng-T ASME 125 (2003) 428–437.
[24] F. Kucuk, M. Karakas, L. Ayestaran, Well testing and analysis techniques for layered reservoirs, SPE Form. Eval. 1 (1986) 342–354.
[25] H. Darcy, The Flow of Fluids through Porous Media, McGraw-Hill, New York, 1937.
[26] N. Rudraiah, B.K. Ramaiah, B.M. Rajasekhar, Hartmann flow over a permeable bed, Int. J. Eng. Sci. 13 (1975) 1–24.
[27] J. McWhirter, M. Crawford, D. Klein, Magnetohydrodynamic flows in porous media II: experimental results, Fusion Technol. 34 (1998) 187–197.
[28] P.J. Prescott, F.P. Incropera, Magnetically damped convection during solidification of a binary metal alloy, J. Heat Tran. 115 (1993) 302–310.
[29] P. Lehmann, R. Moreau, D. Camel, R. Bolcato, Modification of interdendritic convection in directional solidification by a uniform magnetic field, Acta Mater. 46 (1998) 1067–1079.
[30] R.E. Cunningham, R.J. Williams, Diffusion in Gases and Porous Media, Plenum Press, New York, 1980.
[31] K. Das, S. Jana, Heat and mass transfer effects on unsteady MHD free convection flow near moving vertical plate in porous medium, Bull Soc Math Banja Luka 17 (2010) 15–32.
[32] S.S. Das, S.R. Biswal, U.K. Tripathy, P. Das, Mass transfer effects on unsteady hydromagnetic convective flow past a vertical porous plate in a porous medium with heat source, J. Appl. Fluid Mech. 4 (2011) 91–100.
[33] S.S. Das, M. Maity, J.K. Das, Unsteady hydromagnetic convective flow past an infinite vertical porous plate in a porous medium, Int. J. Energy Environ. 3 (2012) 109–118.
[34] S.S. Das, S. Parija, R.K. Padhy, M. Sahu, Natural convection unsteady magneto-hydrodynamic mass transfer flow past an infinite vertical porous plate in presence of suction and heat sink, Int. J. Energy Environ. 3 (2012) 209–222.
[35] S.S. Das, A. Satapathy, J.K. Das, J.P. Panda, Mass transfer effects on MHD flow and heat transfer past a vertical porous plate through a porous medium under oscillatory suction and heat source, Int. J. Heat Mass Tran. 52 (2009) 5962–5969.

[36] C. Fetecau, M. Rana, C. Fetecau, Radiative and porous effects on free convection flow near a vertical plate that applies shear stress to the fluid, Z. Naturforsch. 68 (2013) 130–138.
[37] S.K. Ghosh, O.A. Beg, Theoretical analysis of radiative effects on transient free convection heat transfer past a hot vertical surface in porous media, Nonlinear Anal. Model Contr. 13 (2008) 419–432.
[38] A. Hussanan, Z. Ismail, I. Khan, A.G. Hussein, S. Shaife, Unsteady boundary layer MHD free convection flow in a porous medium with constant mass diffusion and Newtonian heating, Eur Phys J Plus 129 (2014) 46, https://doi.org/10.1140/epjp/i2014-14046-x.
[39] A. Hussanan, M.Z. Salleh, I. Khan, R.M. Tahar, Z. Ismail, Soret effects on unsteady magnetohydrodynamic mixed convection heat-and-mass-transfer flow in a porous medium with Newtonian heating, MaejoInt J Sci Technol 9 (2015) 224–245.
[40] J.C. Maxwell, On the dynamical theory of gases, Phil. Trans. Roy. Soc. Lond. 157 (1867) 49–88.
[41] M.A. Imran, M.B. Riaz, N.A. Shah, A.A. Zafar, Boundary layer flow of MHD generalized Maxwell fluid over an exponentially accelerated infinite vertical surface with slip and Newtonian heating at the boundary, Results Phys 8 (2018) 1061–1067.
[42] N. Iftikhar, S.M. Husnine, M.B. Riaz, Heat and mass transfer in MHD Maxwell fluid over an infinite vertical plate, J Prime Res Math 15 (2019) 63–80.
[43] T. Anwar, P. Kumam, W. Watthayu, Asifa, Influence of ramped wall temperature and ramped wall velocity on unsteady magnetohydrodynamic convective Maxwell fluid flow, Symmetry 12 (2020) 392, https://doi.org/10.3390/sym12030392.
[44] G.S. Seth, M.S. Ansari, R. Nandkeolyar, MHD natural convection flow with radiative heat transfer past an impulsively moving plate with ramped wall temperature, Heat Mass Tran. 47 (2011) 551–561.
[45] N. Narahari, B.K. Dutta, Effects of thermal radiation and mass diffusion on free convection flow near a vertical plate with Newtonian heating, ChemEng Comm 199 (2012) 628–643.
[46] Q. Rubbab, D. Vieru, C. Fetecau, C. Fetecau, Natural convection flow near a vertical plate that applies a shear stress to a viscous fluid, PloS One 8 (2013) 1–7.
[47] J.N. Tokis, A class of exact solutions of the unsteady magneto hydrodynamic free-convection flows, Astrophys. Space Sci. 112 (1985) 413–422.
[48] H. Stehfest, J.W. Goethe, Numerical inversion of Laplace transforms, Commun. ACM 13 (1970) 47–49.